# Graded-reflectivity mirror based on a volume phase hologram in a photopolymer film

Tian-Jie Chen and Ying-Chih Chen

Graded-reflectivity mirrors for 1064-nm wavelength have been fabricated by use of volume phase holograms recorded in photopolymer films. A method for producing such holograms for the 1064-nm radiation by use of a 532-nm light source with a short (0.1-mm) coherence length was developed. The measured peak reflectivity of the mirror reached 95%, and its super-Gaussian profile well matched that calculated based on coupled-mode theory. The mirror can withstand a peak power density greater than $10^8$ W/cm$^2$. This method can also be used for fabricating deflectors that direct an incident beam to any specified angle other than the angle of reflection. 

*OCIS codes:* 090.1970, 090.2890, 230.4040, 050.7330, 160.2900, 230.1480.

## 1. Introduction

Mirrors with specific reflectivities for specified wavelengths are commonly used in lasers and optical systems. Conventional multilayer dielectric films coated upon planar or spherical substrates work well for most applications. New developments in laser technology call for more-sophisticated mirrors. For example, graded-reflectivity mirrors with Gaussian, super-Gaussian, or doughnut-shaped reflectivity profiles are often needed for beam shaping in high-power solid-state lasers with unstable resonators.[1] These graded-reflectivity mirrors can be fabricated by a specially controlled dielectric deposition technique,[2] but the fabrication process is rather costly. A simple and low-cost fabrication process for graded-reflectivity mirrors is desired.

We report the fabrication of graded-reflectivity mirrors based on volume phase holograms recorded in photopolymer films. Optically generated holograms have been widely used in the construction of diffractive optics. Theoretically, a properly designed diffractive optics should be able to reach 100% efficiency.[3] Considerable effort has been devoted to improvement of the fabrication processes with a view to obtaining higher efficiency. For example, the techniques developed in the very large-scale-integrated-circuit industry, such as shaped-beam lithography, variable-energy electron-beam lithography, and gray-scale lithography,[4] were introduced in conjunction with computers for hologram fabrication. Recently, micromachining workstations were developed to generate diffractive optical elements by a direct-writing method.[5] All these techniques have involved many complex and costly steps and required major capital investment. They were more suitable for mass production than for fabricating small quantities of optics for special purposes.

The diffraction efficiency is an important indicator of performance for diffractive optics. It is well known that the phase holograms are inherently more efficient.[3] The theoretical diffraction efficiency for a volume phase hologram working under the Bragg condition is close to unity.[6] However, the commonly used hologram recording media can hardly provide such high efficiency because of their intrinsic deficiencies. According to a recently published survey,[4] the efficiency of diffractive optics achieved before 1997 was approximately 70–80%, which is far below the ideal number of 100%. Silver halide is typically used in holography because of its high photo speed and wide spectral sensitivity. Yet its nonlinear response characteristics, high scattering loss, and wavelength shift caused by wet processing have restricted its use to the cases in which light scattering and wavelength shift can be tolerated. Dichromate gelatin is widely used for holographic optical elements because of its good holographic performance and low scattering. However, it requires wet pro-

The authors are with the Department of Physics and Astronomy, Hunter College of the City University of New York, 695 Park Avenue, New York, New York 10021. (T.-J. Chen's e-mail address is tjchen@shiva.hunter.cuny.edu.)

Received 4 May 1998; revised manuscript received 2 July 1998.
0003-6935/98/286603-06$15.00/0

cessing and also has problems with material variability and environmental instability.

We report the fabrication of holographic graded-reflectivity mirrors for Nd:YAG lasers at a wavelength of 1064-nm by using the newly developed DuPont HRF600X001-20 photopolymer films.[7] Its environmental stability, dry-processing performance, less postprocessing shrinkage, and high refractive-index modulation make this material attractive for use in high-efficiency phase holograms. Because of the insensitivity of the material to 1064-nm radiation, a special configuration was developed that enabled us to fabricate the holograms for the 1064-nm radiation by using a 532-nm light source with a short (0.1-mm) coherence length. The mirror produced by this technique has a graded-reflectivity profile along the radius $r$ and a 95% reflectivity at the center. The measured reflectivity profile of the reflector matches well the profile calculated by coupled-mode theory and also matches a super-Gaussian profile described by $R(r) = R_0 \exp[-(r/w)^n]$, where $R_0$ is the reflectivity at the center, $w$ is the waist, and $n = 3$. This close match opens the door to fabricating mirrors with prescribed profiles by controlling the intensity profile of the laser beam and the time of exposure in the hologram making process. This method can also be used to fabricate reflectors that direct the incident beam to a specified angle other than the angle of reflection with an efficiency close to unity. Our tests show that this mirror can withstand a peak power density greater than $10^8$ W/cm$^2$ for 1-ns laser pulses at a 6-kHz repetition rate at 1064 nm.

## 2. Design

The volume phase hologram is essentially a Bragg reflector. Our goal is to use the volume phase hologram as a mirror at 1064-nm wavelength. Unfortunately, the hologram cannot be made directly with 1064-nm radiation because of the insensitivity of the recording medium to that wavelength. Here we describe a method of fabricating holographic mirrors for 1064-nm radiation by use of a 532-nm light source.

We adopt the following conventions throughout the discussion. All the incident, reflection, and diffraction angles are defined as the angles from the film's surface to the ray. Subscripts 1 and 2 stand for the reference and object beams used in making the hologram and for the incident and diffracted beams used in reconstruction, respectively. Subscripts $a$ and $f$ stand for the parameters in the air and in the film and superscripts $m$ and $w$ stand for the parameters for making and using the hologram, respectively.

It is well known that a volume hologram can be constructed from two beams, 1 and 2 in Fig. 1, incident from opposite sides onto the recording medium with angles $\Theta_{1a}^{(m)}$ and $\Theta_{2a}^{(m)}$, respectively. If both beams are plane waves, then a blank hologram consisting of periodic layers of refractive-index modulation in the film will be generated. The orientation of these layers is in the $\Theta_L = [\Theta_{1f}^{(m)} - \Theta_{2f}^{(m)}]/2$ direction, where $\Theta_{2f}^{(m)}$ and $\Theta_{1f}^{(m)}$ are determined by $\Theta_{2f}^{(m)}$

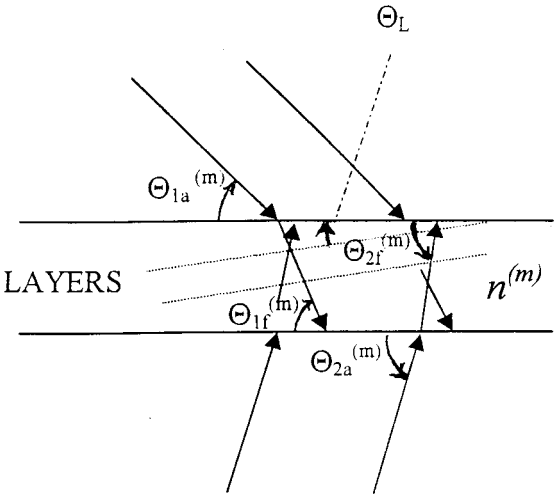


Fig. 1. Schematic of creation of a volume phase hologram.

$= \sin^{-1}\{[1/n^{(m)}]\sin\Theta_{2a}^{(m)}\}$ and $\Theta_{1f}^{(m)} = \sin^{-1}\{[1/n^{(m)}]\sin\Theta_{1a}^{(m)}\}$, respectively, and $n^{(m)}$ is the refractive index of the film. The period of the layer structure, $d$, is

$$d = [\lambda^{(m)}/n^{(m)}](2\sin\{[\Theta_{2f}^{(m)} + \Theta_{1f}^{(m)}]/2\})^{-1}, \quad (1)$$

where $\lambda^{(m)}$ is the wavelength of these beams. When a beam with wavelength $\lambda^{(w)}$ is incident onto this film (Fig. 2) at an angle $\Theta_f'$ (in the film), which satisfies the Bragg condition

$$2d\sin\Theta_f' = [\lambda^{(m)}/n^{(m)}]\sin\Theta_f'(\sin\{[\Theta_{2f}^{(m)} + \Theta_{1f}^{(m)}]/2\})^{-1} = \lambda^{(w)}/n^{(w)}, \quad (2)$$

then a reflected beam will be generated at the same angle $\Theta_f'$ (relative to the layers) in the opposite direction. The angles of these two beams relative to the film, $\Theta_{2f}^{(w)}$ and $\Theta_{1f}^{(w)}$, are determined by

$$\Theta_{1f}^{(w)} - \Theta_{2f}^{(w)} = 2\Theta_L = \Theta_{1f}^{(m)} - \Theta_{2f}^{(m)}, \quad (3)$$

$$\Theta_{2f}^{(w)} + \Theta_{1f}^{(w)} = 2\Theta_f' = 2\sin^{-1}([\lambda^{(w)}n^{(m)}/\lambda^{(m)}n^{(W)}] \times \sin\{[\Theta_{2f}^{(m)} + \Theta_{1f}^{(m)}]/2\}). \quad (4)$$

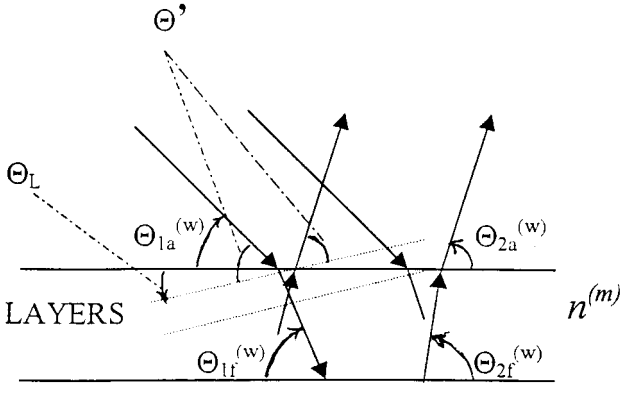


Fig. 2. Volume phase hologram as a deflector.

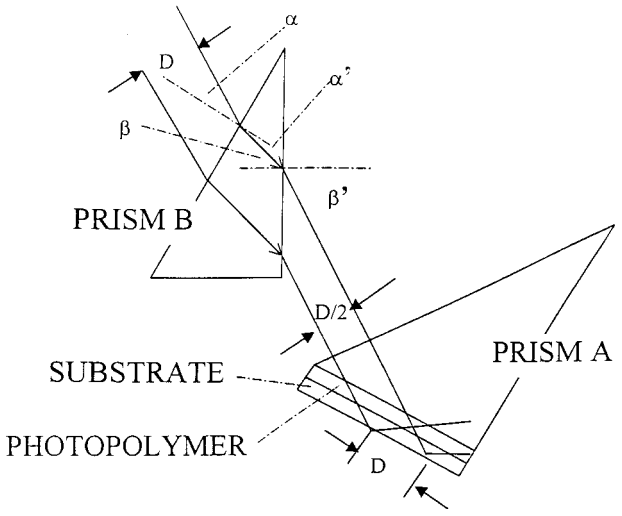


Fig. 3. Schematic of the prism system for making a hologram.

Then the angles of the incident and the diffracted beams in the air are given, respectively, by

$$\Theta_{1a}^{(w)} = \sin^{-1}[n^{(w)} \sin \Theta_{1f}^{(w)}], \quad (5)$$

$$\Theta_{2a}^{(w)} = \sin^{-1}[n^{(w)} \sin \Theta_{2f}^{(w)}]. \quad (6)$$

Equations (3)–(6) are the working equations for design. For a hologram generated by a laser beam of wavelength $\lambda^{(m)}$ at incident angles $\Theta_{1a}^{(m)}$ and $\Theta_{2a}^{(m)}$, the angles $\Theta_{1a}^{(w)}$ and $\Theta_{2a}^{(w)}$ for reconstructing at the wavelength $\lambda^{(w)}$ can be obtained from those equations. In the actual designing process the sequence is reversed: The reconstructing angles are given first, and the angles for making the hologram are to be determined. Note that these formulas are reversible: If a hologram is made with incident angles $\Theta_{1a}^{(m)}$ and $\Theta_{2a}^{(m)}$ at wavelength $\lambda^{(m)}$, the working angles for wavelength $\lambda^{(w)}$ are $\Theta_{1a}^{(w)}$ to $\Theta_{2a}^{(w)}$. If a hologram is made with incident angles $\Theta_{1a}^{(w)}$ and $\Theta_{2a}^{(w)}$ at wavelength $\lambda^{(w)}$, the working angles for $\lambda^{(m)}$ will be exactly the same as $\Theta_{1a}^{(m)}$ and $\Theta_{2a}^{(m)}$. Therefore one can use these formulas to calculated the angles for making the hologram.

The mirror reported here is fabricated by use of a 532-nm laser beam to reflect a 1064-nm laser beam at normal incidence. In this case we have $\Theta_{1a}^{(m)} = \Theta_{2a}^{(m)} = \Theta_{1f}^{(m)} = \Theta_{2f}^{(m)} = 90°$. From Eq. (1), the required period of the refractive-index modulation is $d = \lambda_m/2n_m = 1064 \text{ nm}/2n_m$. If the difference in the refractive indices for the two wavelengths is taken into account, the angles of the 532-nm beam in the film are found from Eqs. (3)–(6) to be $\Theta_{1f}^{(w)} = \Theta_{2f}^{(w)} = \sin^{-1}[n^{(1064)}/2n^{(532)}] \approx 30°$. Other factors, such as the shrinkage and the diffractive-index change in the film in processing, will modify the angles by a few minutes of arc. We address these problems in Section 3. According to Snell's law, the beams that make a 30° angle in the film cannot be generated by direct incidence from air. Prism A (Fig. 3) is used to guide the beam into the film. The light that is normally incident upon the hypotenuse will strike the shorter side of prism A at an angle $\Theta_{1f}^{(w)} = 30°$; we can adjust it by causing the incident beam to deviate from its normal direction. The photopolymer film is laminated upon the prism. The measured refractive index of the prism is 1.517, and the refractive index of the photopolymer film is 1.516 at 514 nm, as specified by the manufacturer. Thus the interface is nearly index matched, and the light that is normally incident upon the hypotenuse will propagate in the film at an angle $\Theta_{1f}^{(w)} = 30°$, as required. The substrate is a polymer film with a thickness of 60 μm and a refractive index close to that of the film. The incident beam, after passing through the photopolymer, enters transparently into the substrate and undergoes total internal reflection at the substrate–air interface. The totally reflected beam then interferes with the incident beam at an angle $\Theta_{1f}^{(w)} = \Theta_{2f}^{(w)} = 30°$. These two beams will interfere with each other and generate a set of interference layers in the photopolymer film.

The present system has two major advantages: First, the experimental setup is insensitive to mechanical vibrations because there are no movable parts in the optical path. Second, because of the small optical path-length difference between the two interfering beams, the required coherence length of the light source will be <0.1 mm.

Because of the geometry, a beam with a round cross section, after it passes through the hypotenuse and then arrives at the photopolymer film, will be distorted into an elliptical shape with a major axis/minor axis ratio of 2. To correct for this effect, the beam is first compressed in the incident plane by prism B before it enters prism A. The compression ratio is given by

$$M = \cos \alpha' \cos \beta' / \cos \alpha \cos \beta, \quad (7)$$

where α and β are the incident angles and α′ and β′ are the deflection angles at the first and the second surfaces of prism B, respectively. To compress the beam by a factor of 2, we set $M = 0.5$ and the incident angle α′ at 11.1° for the $n = 1.517$ prism.

The hologram consists of layers of periodic refractive-index modulation whose spatial dependency can be described as

$$n(z) = n_0 + \Delta n \sin 2\pi z/d, \quad (8)$$

where $d$ is the period of the refractive-index modulation along $z$, the normal of the layers, which is the normal to the film in our case, and $\Delta n$ is the depth of the refractive-index modulation. According to coupled-mode theory,[6] the reflectivity of such a periodic structure can be described by

$$R = \tanh^2[2\pi \Delta n L/\lambda^{(m)}], \quad (9)$$

where $L$ is the thickness of the film. According to the manufacturer's specifications, $\Delta n = 0.03$ and $L = 20$ μm, and the calculated peak reflectivity is 99.5%. If a beam with a Gaussian profile $I = I_0 \exp(-r^2/w^2)$, where $w$ is the waist of the Gaussian beam and $r$ is

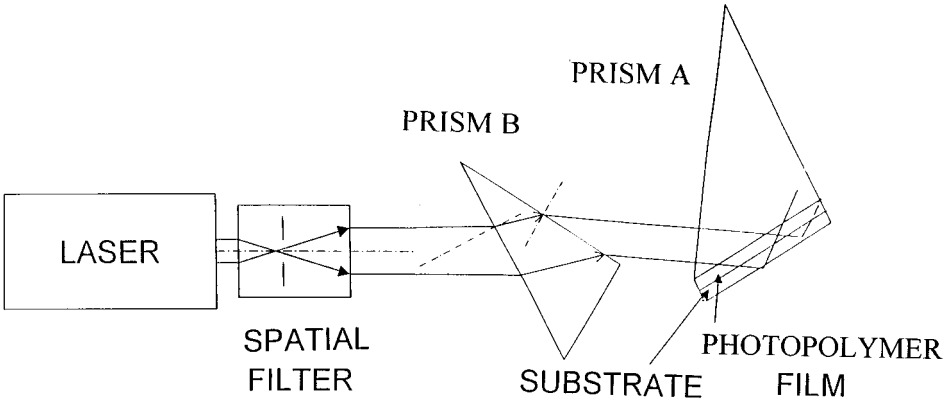

Fig. 4. Schematic of the experimental setup.

the distance from the center of the beam, is used in generating the hologram, the profile of the reflectivity should be

$$R = \tanh^2\{2\pi\Delta n[\exp(-r^2/w^2)]L/\lambda^{(m)}\}. \quad (10)$$

Here the modulation of the refractive index is assumed to be linearly proportional to the intensity of the beam. Therefore the reflectivity will depend on $r$, and the profile will be determined by the beam's profile. Inasmuch as the Gaussian distribution function appears as the argument of a hyperbolic tangential function in Eq. (10), the reflectivity profile of the film will not remain Gaussian. The numerical calculation shows that it is super-Gaussian. If the film is overexposed, the response of the film can be nonlinear and the saturation can lead to a flat reflectivity profile. Because the intensity varies slowly with radius at the central portion of a Gaussian beam, a strongly expanded Gaussian beam can be used to generate a flat profile too, if only the central part of the beam is used.

### 3. Experiments and Results

The experimental setup is shown in Fig. 4. A Uniphase μGreen laser emitting at 532 nm was used as the light source. The bandwidth of the laser was $<0.1$ nm, corresponding to a coherence length of $>2.5$ mm. After it passed through a spatial filter, the beam was collimated into a parallel Gaussian beam with a waist of $w \approx 3$ mm. The beam was then compressed by prism B before entering prism A, which guided the beam into the photopolymer film and then into the substrate. The incident and the reflected beams from the substrate–air interface created interference fringes in the photopolymer film. The thickness of the substrate was 60 μm. Therefore the path difference between the two beams was $2 \times 80\ \mu\text{m} \times \sin 30° = 80\ \mu\text{m}$, which was the required minimum coherence length for the light source and is much less than the coherence length of the laser that we used in this experiment.

The laser power that fell upon the film was ~1 mW. The spot size was $w \approx 3$ mm. DuPont HRF-600x001-20 holographic recording photopolymer films were used as the recording material. The exposure time was 1–2 min. After exposure, the film was exposed to 365-nm UV radiation for 2 min. The intensity of the UV beam was ~2 mW/cm$^2$. After curing, the film was baked at 120 °C for 2 h.

A transmission spectrum of the finished holographic reflector was measured by a Nicolet 760 Fourier-transform infrared spectrometer. The measured curve is shown in Fig. 5. The curve exhibits a flat bottom centered at 1070 nm. It corresponds to a reflection peak at this wavelength. The difference between the measured transmission minimum at 1070 nm and the designed value at 1064 nm is 0.8%.

The reflectivity of the film was measured at normal incidence at 1064 nm. The result is shown in Fig. 6(a). The peak reflectivity was 95.1%, which corresponds to a reflectivity at peak wavelength of 95.9%. According to the manufacturer's specification, the maximum refractive-index change was $\Delta n = 0.03$, which corresponded to a calculated reflectivity of 99.5% at peak position. Our result was slightly

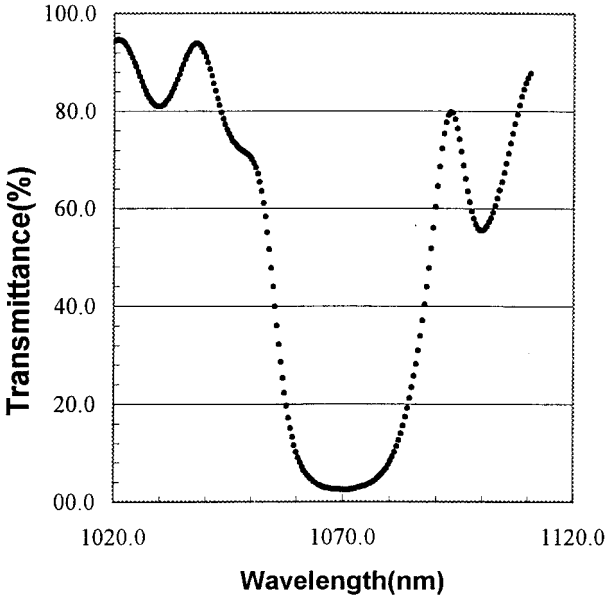

Fig. 5. Transmittance of the reflector.

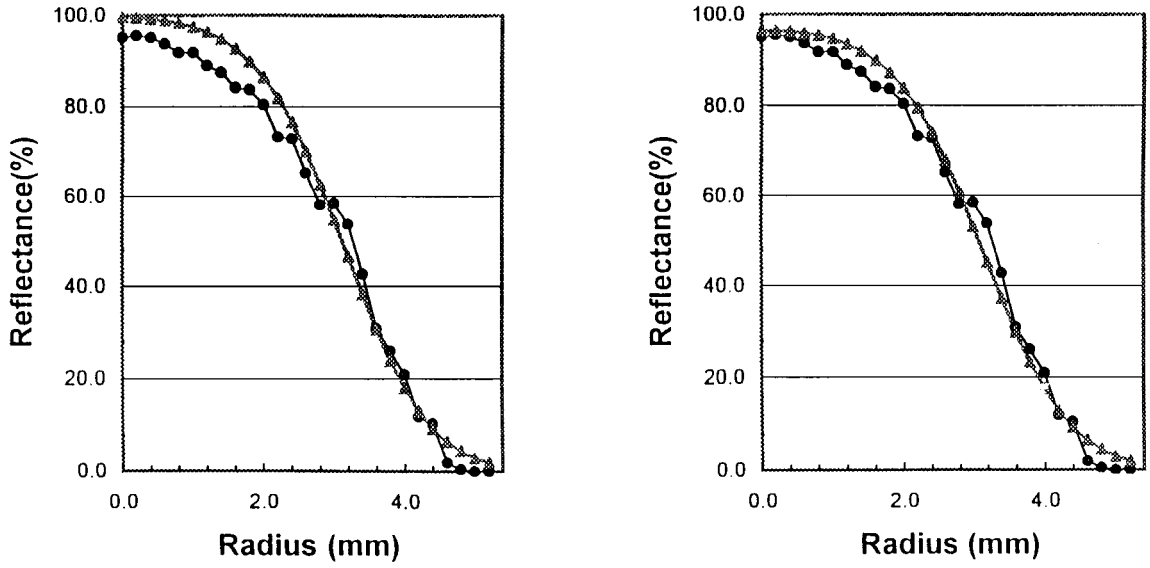


Fig. 6. Measured (filled circles) and calculated (filled triangles) reflectivity profiles (a) with $\Delta n = 0.03$ and (b) with $\Delta n = 0.023$.

lower than the calculated value. An infrared absorption measurement showed that the film was transparent at a 1064-nm laser wavelength, and the absorption was less than 1% for the thickness of our film with its substrate. The lower reflectivity is attributed to the smaller depth of the index modulation as specified by the manufacturer. The index modulation of $\Delta n = 0.03$ provided by the manufacturer is for the visible region. It is expected that the index modulation will decrease in the infrared region. If a smaller value of $\Delta n = 0.023$ is adopted, then the calculated reflectivity profile matches the measured one well, as shown in Fig. 6(b).

Our numerical computation shows that the measured profile based on Eq. (10) is close to a super-Gaussian profile described by

$$R = R_0 \exp[(-r/w)^3], \tag{11}$$

where $w = 3.5$ mm. The measured and calculated super-Gaussian curves are plotted in Fig. 7.

The peak reflectivity obtained in the present study is considerably higher than the previously reported peak of 70–80%.[4] The good match between the measured and the calculated reflectivity profiles illustrates that the diffractive optics made by our approach can reach the efficiency predicted by coupled-mode theory. When the exposure is in the linear regime, the reflectivity profile is close to super-Gaussian, with $n = 3$. Other specially tailored reflectivity profiles can be obtained by overexposure or by use of the central part, which is nearly flat, of a Gaussian beam. As an example, we generated a reflector with a nearly flat reflectivity profile by expanding the laser beam, and only the central part of the laser beam was used in generating the hologram. The resultant reflectivity profile is nearly flat, as shown in Fig. 8.

The optical damage threshold of the film was also tested with a 1064-nm 1-ns pulsed laser with a 6-kHz repetition rate. No damage was found at a peak power density of $10^8$ W/cm$^2$.

It is well known that the refractive index $n$ as well as the film thickness $t$ can change after processing.

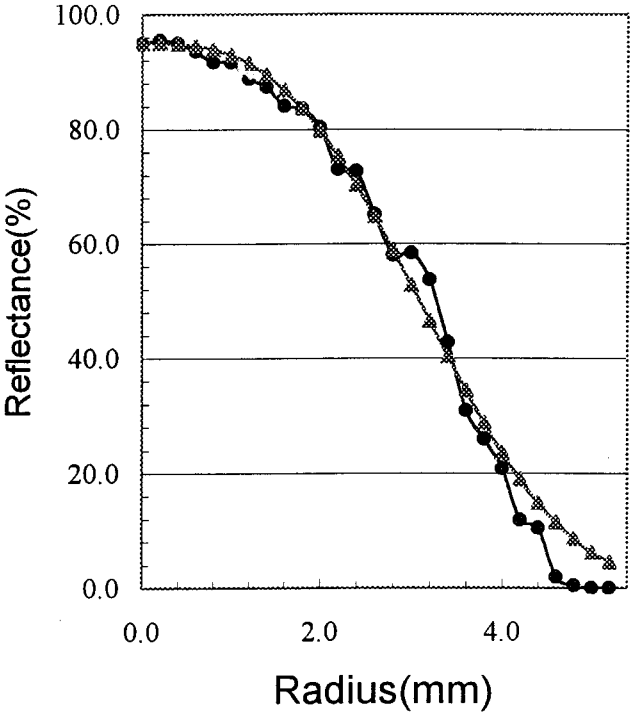


Fig. 7. Measured (filled circles) and calculated (filled triangles) super-Gaussian profiles.

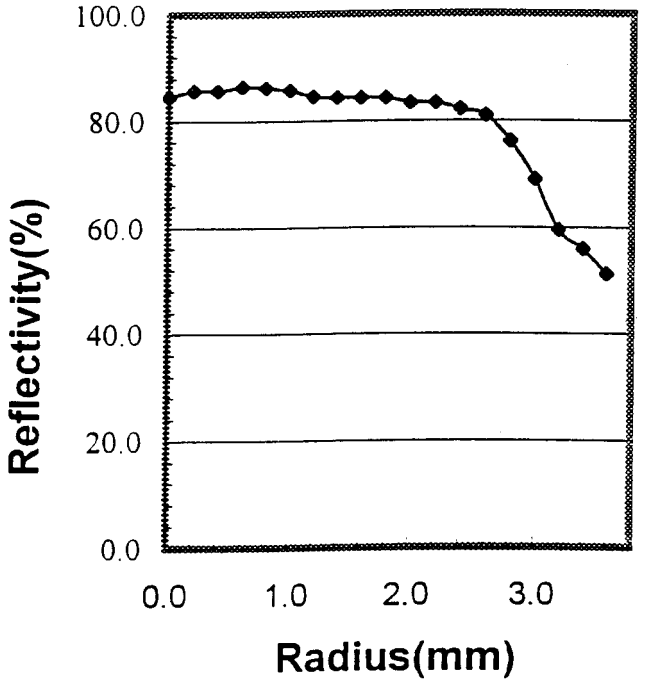


Fig. 8. Reflectivity of a mirror with a flat profile.

The peak wavelength of reflectivity is proportional to the optical thickness $nt$. Gambogi *et al.*[7] reported a blueshift of the playback wavelength in HRF-600 film. In their case the refractive index $n$ increased 1.8% and the thickness $t$ was reduced by 4.8% at 514 nm. The net result is a blue peak shift of $\Delta\lambda/\lambda = -2.6\%$. To measure the changes of the optical thickness $nt$ of the photopolymer film at 1064 nm before and after processing we measured the modulation period of the interference fringes in the transmission spectrum obtained with a Fourier-transform infrared spectrometer. To eliminate the interference caused by the substrate we peeled the substrate off from the fresh (without laser exposure, UV curing, and baking) film. Special care was taken to avoid any stretching of the film during peeling. First the optical thickness was measured from the interference fringes for the fresh film. Then the same film was exposed to laser light, subjected to UV curing, and finally baked for 2 h at 200 °C. The optical thickness was then measured again. Our data show a change of +1.5% instead of a negative value, which suggests that the refractive-index change in this spectral region is so large that it is more than enough to offset the effect of shrinking, resulting in a net positive change of $nt$. This result implies that the peak wavelength should shift toward the red by 1.5% instead of by 0.8% as measured. Because the reflector was made by a 532-nm laser and works at 1064 nm, the dispersion of the refractive index will affect the optical thickness. No dispersion data were available for this film. The normal dispersion will shift the reflection peak toward the short-wavelength side. Our experiment suggests that the dispersion will be approximately 1–2% in this region for the film if possible measurement error is taken into account.

In summary, we have designed and fabricated low-cost graded-reflectivity mirrors for 1064-nm wavelength with a graded reflectivity and 95% reflectivity at the center, using volume phase holograms recorded in photopolymer films. The holograms were fabricated for 1064-nm radiation by use of a 532-nm light source with a short coherence length. The measured profile of the reflectivity well matches that of the calculated profile, based on coupled-mode theory and also on a super-Gaussian profile with $n = 3$. The reflector can withstand greater than $10^8$-W/cm$^2$ power density. This method can also be used for fabricating mirrors for directing a beam to a specified angle other than the angle of reflection.

This study was supported by the New York State Center for Advanced Technology on Ultrafast Photonic Materials and Applications at the City University of New York.

### References

1. W. Koechner, *Solid-State Laser Engineering*, 4th ed. (Springer-Verlag, New York, 1994), Chap. 5.
2. G. Duplain, P. G. Verly, J. A. Dobrowolski, A. Waldorf, and S. Bussiere, "Graded-reflectance mirrors for beam quality control in laser resonators," Appl. Opt. **32,** 1145–1167 (1993).
3. C. B. Burckhardt, "Efficiency of dielectric grating," J. Opt. Soc. Am. **57,** 601–603 (1967).
4. M. B. Fleming and M. C. Hutley, "Blazed diffractive optics," Appl. Opt. **36,** 4635–4643 (1997).
5. G. P. Behrmann and M. T. Duignan, "Excimer laser micromachining for rapid fabrication of diffractive optical elements," Appl. Opt. **20,** 4666–4674 (1997).
6. A. Yariv and P. Yeh, *Optical Wave in Crystals* (Wiley, New York, 1983), pp. 177–188.
7. W. J. Gambogi, A. M. Weber, and T. J. Trout, "Advances and applications of DuPont holographic photopolymers," in *Holographic Imaging and Materials*, T. H. Jeong, ed., Proc. SPIE **2043,** 13–25 (1993).